PAPER

Check for updates

Free volume dependence of the dielectric constant of poly(vinylidene fluoride) nanocomposite films†

Lei Yang, [ab] Xuyang Liu, [a] Zhouxun Lu, [a] Tong Song, [a] Zhihong Yang, [a] Jianmei Xu, [a] Wei Zhou, [ID] *[ab] Xingzhong Cao, [ID] [c] Runsheng Yu[c] and Qing Wang [ID] [d]

The free volume effects on the dielectric properties of the polymer are ambiguous, and the quantitative effect of free volume on the dielectric properties has rarely been systematically studied, especially in the high-elastic state dipolar (HESD) polymer. In this work, the free volume of dipolar poly(vinylidene fluoride) (PVDF) is regulated by the addition of Al_2O_3, which greatly increase the size of free volume holes. Then the effect of free volume on the dielectric properties of $PVDF/Al_2O_3$ composites is discussed. The greatly enlarged size of free volume holes is believed to potentially generate disparate effects on dielectric constant under different frequencies in such kinds of HESD polymer-based composites, bringing about more remarkable frequency dependence of the dielectric constant. The influence of atomic-scale microstructure based on free volume further clarifies the free volume effects on the dielectric properties and provides valuable insights for the research of dielectric behaviour of polymer composites, which is constructive to design novel dielectric materials and further optimize the dielectric properties of dipolar dielectric polymer composites.

1. Introduction

The polymer dielectrics display vast potential applications in power systems and hybrid vehicles.[1–4] Dipolar polymers such as PVDF and PVDF-based copolymers serve as promising polymer dielectrics for high energy density capacitors.[5] However, polymer dielectrics suffer from intrinsically limited dielectric properties to meet the need of practical applications. Consequently, polymer-based nanocomposites are widely developed to obtain dielectrics with more superior dielectric properties. Typically, kinds of fillers[6–8] were employed for polymer-based dielectrics. Subsequently, the structural design of sandwich-structured composites[9,10] was ingeniously adopted to achieve concomitantly enhanced dielectric constant and breakdown strength. The inorganic layer was also introduced to act as an insulating layer for improving dielectric properties and energy storage performances.[11–13] Despite conspicuous progress having been achieved, it is still challenging to use these dielectrics in practical applications due to some limitations.

Beyond that, the microstructure effect on dielectric properties in dielectrics has attracted more attention recently. Zhang

et al.[14,15] found that the increased free volume could contribute to the enhancement of dielectric constant in dipolar glass polymers, which contain strongly polar groups. They adjusted the free volume of polymer *via* ultralow filler loading or blending with other polymers, and observed the enhanced dielectric constant due to the increased free volume, which illustrates that the effect of free volume is non-negligible. However, this discussion of free volume contribution to the dielectric constant was based on qualitative information of free volume and on account of glassy dipolar polymers. Conversely, some other previous works[16–20] present that the dielectric constant of polymers are reduced by enlarging the free volume. Hence, the free volume effect on the dielectric constant of polymer is still ambiguous and rarely discussed in HESD polymer, *e.g.* dipolar PVDF. As known, the high dielectric constant of dipolar polymers essentially originates from the orientation polarization of intrinsic dipoles, which relies on the motion state of molecular chains and the motion space endowed by free volume holes.[21] Particularly, the glass transition temperature of PVDF is between −40 °C and −30 °C (ref. 5) and in high-elastic state at ambient temperature, representing the intense molecular motion and resultant large free volume. Therefore, it can be inferred that the dielectric constant of PVDF may be more sensitive to the free volume variation. For the design of next generation dielectrics and optimization of dielectric performances, it is of vital necessity to quantitatively discuss how the free volume affects the dielectric constant in such kind of HESD polymer like PVDF.

The free volume theory of polymers developed by Fox and Flory *et al.*[22–24] is based on the idea that the motion of molecules

[a]Faculty of Materials Science and Chemistry, China University of Geosciences, Wuhan 430078, China. E-mail: weizhou@cug.edu.cn

[b]Zhejiang Institute, China University of Geosciences, Hangzhou 311305, China

[c]Institute of High Energy Physics, Chinese Academy of Sciences, Beijing 100049, China

[d]Department of Materials Science and Engineering, The Pennsylvania State University, University Park, PA 16802, USA

in the bulk state is dependent on the existence of holes. Positron annihilation lifetime spectroscopy (PALS) is well recognized as a unique method to determine and reflect the free volume of polymers. In previous works,[25–28] PALS has been widely utilized to determine the free volume information of polymer and polymer composites. The introduction of nanofiller into polymers is an efficient approach to regulate the free volume of polymer materials.[29,30] In this work, Al_2O_3 is adopted as the filler to fabricate $PVDF/Al_2O_3$, because the dielectric constant of Al_2O_3 is approximate to that of pristine PVDF, minimizing the impact of interfacial polarization. Moreover, the hydroxyl groups existing on surfaces of Al_2O_3 particles tend to form hydrogen bonds with PVDF, which tend to induce the free volume variation. In this way, the fluctuation of dielectric constant of PVDF-based composite films induced by free volume variation is believed to be more sensitive and detectable. Different from previous works,[14–20] it is found that the size variation of free volume holes tends to generate dissimilar effects on the dielectric constants at low and high frequencies in high-elastic state dipolar PVDF.

2. Experimental

2.1. Preparation of $PVDF/Al_2O_3$ films

$PVDF/Al_2O_3$ composite films were prepared through tape casting method from N,N-dimethyl formamide (DMF, >99.5%, GC, Aladdin, China) solution of PVDF and Al_2O_3. Commercial PVDF powder was purchased from Arkema Industrial Incorporation (Kynar 761A, M_w = 50–60w, French). Al_2O_3 of α-phase was purchased from Aladdin Industrial Incorporation (99.99% metals basis, Shanghai, China). Firstly, the desired amount of Al_2O_3 powder was dispersed in 20 mL of DMF under ultrasonic agitation for 2 h using Ultrasonic Cleaners JP-020 (40 kHz, Shenzhen, China). The sonication frequency and power are 40 kHz and 100 W, respectively. Then 1 g of PVDF powder was added into Al_2O_3 solution and magnetic stirred for 12 h to obtain a homogeneous hybrid solution. During this process, the receptacle for solution was sealed to avoid water absorption. Then the hybrid solution was cast on a clean glass plate and dried in a vacuum oven at 40 °C for 24 h. Finally, the films were peeled off from glass plates for further use. Al_2O_3 volume contents in $PVDF/Al_2O_3$ films are 0 vol%, 10 vol%, 20 vol%, 30 vol% and 40 vol%, respectively. For simplicity, the PVDF composite film with 10 vol% Al_2O_3 is denoted as PVDF/10AO and the similar abbreviation for other samples. The preparation processes of pristine PVDF and PVDF/AO films are displayed in Scheme 1.

2.2. Characterization

XRD patterns were acquired on Bruker D8-ADVANCE (Bruker, Germany) equipped with Cu Kα radiation ($λ$ = 1.54 Å) and the voltage and current of the instrument are 40 kV and 40 mA, respectively. All film samples were sheared into a relatively regular shape for measurement. The data was recorded over the range of 5° to 90°, 0.5 s per step and the step of 0.02°. FTIR analysis was performed on Fourier Transform Infrared Spectrometer, Thermo Fisher Nicolet iS50 (USA) and the transmission information was collected. The film samples were brittle broken with liquid nitrogen and the cross sections of film samples were examined with scanning electron microscope (SEM), Hitachi SU8010, Japan. TEM image of AO powder is obtained on transmission electron microscopy, JEM-3010, Japan.

PALS measurement was performed to determine the free volume information of polymer nanocomposites. The measurements for the samples at ambient temperature and elevated temperatures were respectively performed on a conventional fast–fast and fast–slow coincidence lifetime spectrometer, and the lifetime spectrometer for high temperature measurement is equipped with Lakeshore DT670 sensor and 335 temperature controller. The corresponding time resolution of the lifetime spectrometer is 250 ps and 210 ps in full width at half maximum (FWHM), respectively. A 10 μCi^{22}Na source was used and pinched by two identical samples during the measuring process. For each sample of PVDF/AO composite films, two lifetime spectrums are collected with a total count of 10^6 for each spectrum. For the positron lifetime measurements of PVDF film at elevated temperatures, two lifetime spectrums are collected with a total count of 2×10^6 for each spectrum. Analysis of positron lifetime spectrums is performed with the finite-term lifetime analysis PATFIT[31] and LT9.0 programs.

Three components ($τ_1$, $τ_2$ and $τ_3$) are obtained from each spectrum for discrete analysis. The long-lived $τ_3$ is on account of the o-Ps pick-off annihilation, which occurs in free volume holes.[32] Assuming that the free volume holes are spherical, the
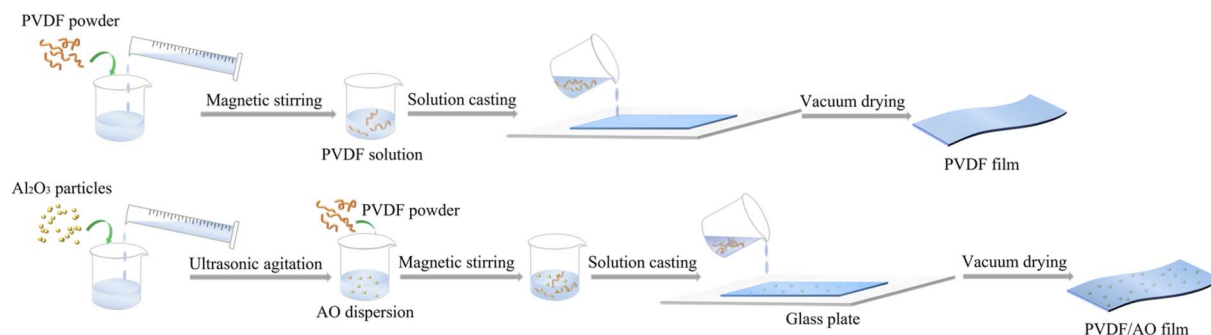
Scheme 1 Preparation processes of pristine PVDF and PVDF/AO films.

average radius (R) and volume (V) of single free volume hole can be obtained from eqn (1) and (2), respectively:[33]

$$\tau_3 = \frac{1}{2}\left[1 - \frac{R}{R+\Delta R} + \frac{1}{2\pi}\sin\left(\frac{2\pi R}{R+\Delta R}\right)\right]^{-1} \quad (1)$$

$$V = \frac{4}{3}\pi R^3 \quad (2)$$

where R is the average radius of single free volume hole and ΔR with a known value of 0.1656 nm.[34,35]

Dielectric spectrums were acquired in the frequency range from 10^3 to 10^7 Hz with the instrument of Align Impedance Analyzer E4990A, USA. The clamp fixture used for the samples was High Temperature Dielectric Measurement System HDMS-1000, Partulab, China. Gold was sputtered on both sides of samples prior to the measurement. The polarization–electric field (P–E) loops were collected under 10 Hz on Radial precision LC ferroelectric tester, Radiant, USA.

3.   Results and discussion

The XRD patterns of AO powder, pristine PVDF film and PVDF/AO composite films are shown in Fig. 1(a). The characteristic peaks of α-phase of PVDF appear at 18.4° and 39° corresponding to the crystal plane (020) and (002), and the characteristic peak at 20.1° is probably attributed to the overlap of characteristic peaks of α-phase and β-phase, which appear at 19.9° at 20.3° respectively.[21,36–39] The FTIR spectrums of AO powder, pristine PVDF and

PVDF/AO composite films are shown in Fig. 1(b). As the intensity of absorption peaks is extremely weak compared with PVDF, the FTIR spectrum of AO is exhibited in Fig. 1(c), confirming the existence of hydroxyl groups on the surface of AO particles. As shown in Fig. 1(b), the characteristic peaks of different crystal forms of PVDF appear in the spectrums. The absorption peaks at 1400, 877 and 480 cm^{-1} correspond to the α crystal form of PVDF[39,40] and the absorption peak at 1166 cm^{-1} is assigned to the β-phase.[40] The absorption peaks at 1232, 835, 512 and 431 cm^{-1} are assigned to the γ-phase. Besides, the absorption peak at 1071 cm^{-1} is ascribed to the wagging of –CH$_2$ groups.[40] As the intensity of absorption peaks of AO is weak, the absorption peaks of AO are not obviously observed in the spectrums of PVDF-based composite films. The morphology of PVDF/AO composites are displayed in Fig. S1.† As seen in Fig. S1(a),† the original AO powder is endowed with spherical-like morphology and the diameter of 20–30 nm. The cross section of pristine PVDF film displays relatively smooth and dense morphology, which is shown in Fig. S1(b).† In Fig. S1(c)–(f),† the AO nanoparticles are well dispersed in the continuously self-connected PVDF matrix, and the cross-sections of PVDF/AO composite films displays rough morphologies due to the addition of AO filler.

The o-Ps lifetime τ_3 and average free volume hole radius of PVDF/AO composites are displayed in Fig. 2. As shown, the o-Ps lifetime τ_3 of pristine PVDF is 2.44 ns, which is in the general range of polymers. After AO filler is introduced into PVDF, the o-Ps lifetime τ_3 and the corresponding free volume hole radius of PVDF are obviously enlarged, which is in accordance with the
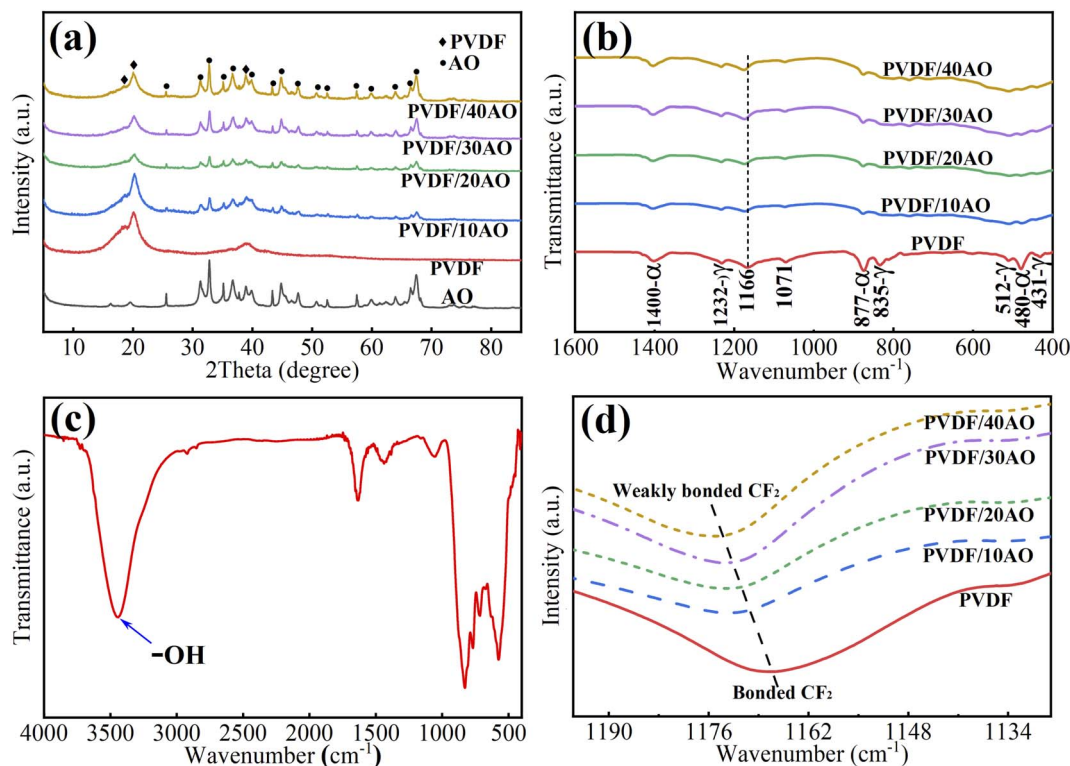

Fig. 1   (a) XRD patterns of PVDF/AO composite films. (b) FTIR spectrums of PVDF/AO composites in the range of 4000–400 cm^{-1}. (c) The FTIR spectrum of AO particles, confirming the existence of hydroxyl groups on the surface of AO particles. (d) The wavenumber shift of CF$_2$ group, confirming the weakened hydrogen bonding in PVDF/AO composites compared to pristine PVDF.
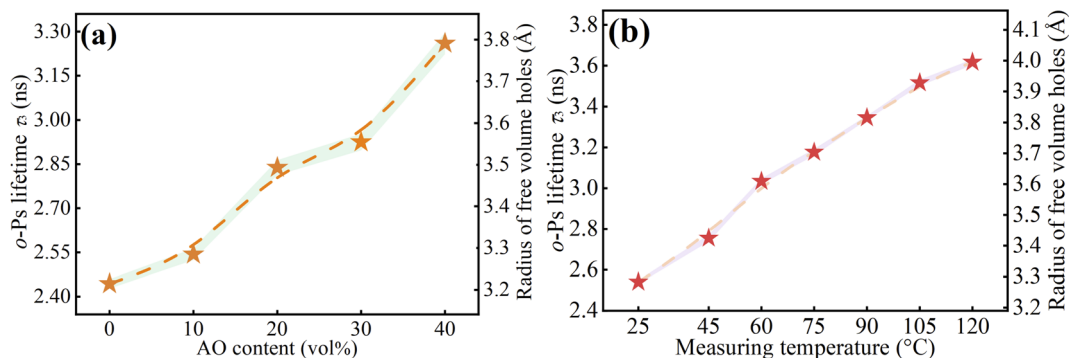
Fig. 2 (a) AO content dependence of o-Ps lifetime τ_3 and free volume radius for PVDF/AO composites. (b) Temperature dependence of o-Ps lifetime τ_3 and free volume radius for pristine PVDF. The lines are drawn to guide eyes.

previous work.[41] The increase of o-Ps lifetime τ_3 and free volume radius is presumably ascribed to the following statements. The addition of AO filler disrupts the stacking pattern of partial molecular segments of the matrix, and the filler was embedded in tightly packed molecular segments. In addition, the hydroxyl groups existing on AO filler surfaces,[42] evidenced in Fig. 1(c), tend to form hydrogen bonding with fluorine atoms of PVDF at the interfaces between AO particles and PVDF matrix. This is evidenced by the position shift of absorption peaks at 1166 cm^{-1} ($-CF_2$) observed in FTIR spectrums, as presented in Fig. 1(d), which implies the weakening of hydrogen bonding in adjacent PVDF molecular chains between hydrogen and fluorine atoms (see Fig. S2† for schematics of hydrogen bonding in PVDF),

indicating that the addition of AO filler disrupts the hydrogen bonding of PVDF polymer and reduces the constraint on PVDF dipoles.[15] The softening of hydrogen bonding in PVDF is advantageous for the motion of molecular chains, thus increasing the o-Ps lifetime τ_3 and free volume radius.[43–45] Fig. 2(b) presents the temperature dependence of o-Ps lifetime τ_3 and free volume radius in pristine PVDF, which will be discussed in the follows.

Fig. 3(a) displays the dielectric spectrums of pristine PVDF and PVDF/AO composite films. It is interesting that the PVDF/AO composites with the increment of AO content exhibits greatly different dielectric constants at low and high frequency. At low frequency, taking 1 kHz for instance, with the increment
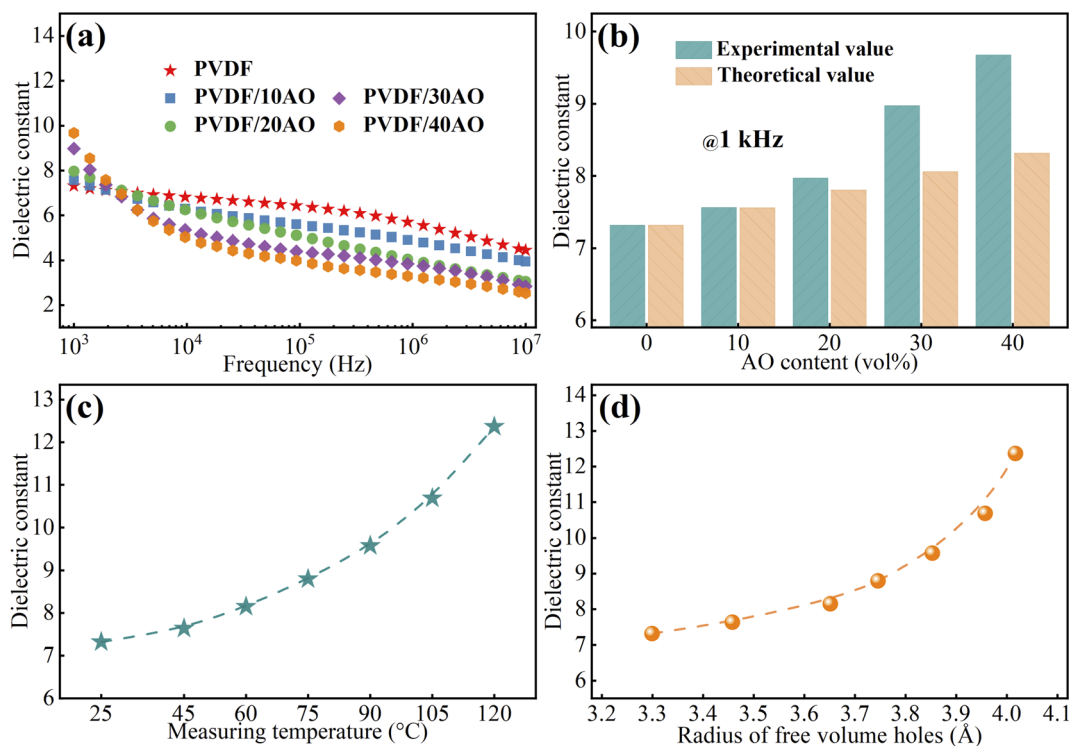

Fig. 3 (a) Dielectric spectrums of PVDF/AO composites with different AO contents. (b) Comparison of experimental and theoretical dielectric constant of PVDF/AO composite films at 1 kHz. (c) The dielectric constant of pristine PVDF as a function of temperature. (d) The free volume radius dependence of dielectric constant in pristine PVDF. The lines are drawn to guide the eyes.

of AO loading, the dielectric constant of PVDF/AO composite film is enlarged as well. However, at high frequency, taking 10 MHz as example, the dielectric constant of PVDF/AO composite films decreases as AO loading increases, exhibiting a converse trend *versus* AO loading. This phenomenon is also observed in previous works.[46,47] To explore this intriguing phenomenon, the theoretical dielectric constant of PVDF/AO composite films with different filler contents was firstly predicted from the applicative theoretical model. Here, as the interaction of adjacent AO nanoparticles are non-negligible when the addition content is high, the Jayasundere–Smith equation[5,48,49] is utilized cause this equation has taken the interaction of nearby fillers into account, which is written as follows:

$$\varepsilon_c = \frac{v_m\varepsilon_m + v_f\varepsilon_f\left[\dfrac{3\varepsilon_m}{\varepsilon_f + 2\varepsilon_m}\right]\left[1 + \dfrac{3v_f\left(\varepsilon_f - \varepsilon_m\right)}{\varepsilon_f + 2\varepsilon_m}\right]}{v_m + v_f\left[\dfrac{3\varepsilon_m}{\varepsilon_f + 2\varepsilon_m}\right]\left[1 + \dfrac{3v_f\left(\varepsilon_f - \varepsilon_m\right)}{\varepsilon_f + 2\varepsilon_m}\right]} \quad (3)$$

where ε_m, ε_f and ε_c represent the dielectric constant of polymer matrix, filler and polymer composite, respectively, and v_f represents the volume content of the filler.

The dielectric constant of AO was obtained from the reported values in the literature[50] and experimental measurement. The experimental and theoretical dielectric constant of PVDF/AO composites at 1 kHz were then compared in Fig. 3(b). Typically, the dielectric constant of polymer composites will be increased due to the interfacial polarization occurring at the interfaces between the polymer matrix and inorganic fillers. As shown in Fig. 3(b), the experimental dielectric constant is higher than the theoretical value, and the deviation is more obvious as the filler content increases. Especially, the dielectric constant of PVDF/40AO composite film even exceeds those of pristine PVDF and Al_2O_3 filler at 10^3 Hz, implying that the enhancement of dielectric constant was not just ascribed to interfacial polarization. As mentioned in previous works,[14,15] the increased free volume could contribute to the enhancement of dielectric constant. Thus, the larger dielectric constant than the theoretical value probably originates from the increased radius of free volume holes displayed in Fig. 2(a). This is considered as the positive effect of free volume holes on dielectric constant at low frequency. To confirm this, the size of free volume holes for pristine PVDF is adjusted at elevated temperatures, which is shown in Fig. 2(b). The corresponding dielectric constant at elevated temperatures is also measured and displayed in Fig. 3(c). As shown in Fig. 2(b), the free volume radius is greatly increased with the elevation of temperature, which is in accordance with the typical temperature dependence of *o*-Ps lifetime in kinds of polymers,[51,52] originating from the strengthened molecular motion motivated by the high temperature. Correspondingly, as exhibited in Fig. 3(c), the dielectric constant of PVDF is also increased with the elevation of temperature. The dielectric constant and free volume radius in pristine PVDF at elevated temperatures are correlated in Fig. 3(d), implying the strong dependence of dielectric constant *versus* the free volume radius, which stems from the more sufficient orientation polarization of intrinsic dipoles due to the enlarged size of free volume holes.[53] This verifies the positive effect of free volume
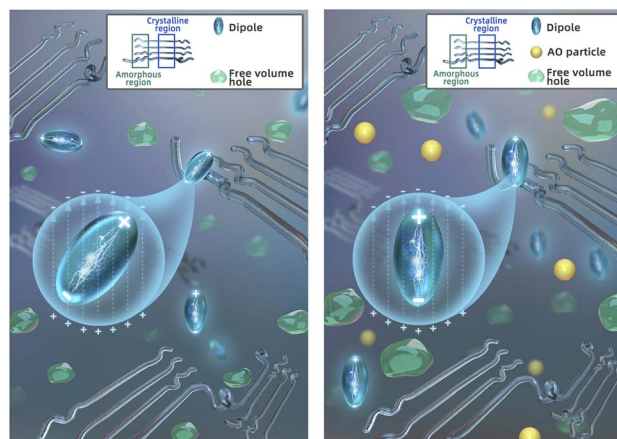
Scheme 2 (a) Orientation polarization of intrinsic dipoles in pristine PVDF. The external electric field are vertically oriented. The dipoles are randomly oriented and orientation polarization is insufficient. (b) Increased orientation polarization of intrinsic dipoles in PVDF/AO composites due to the increased free volume hole size. The dipoles are more parallel to the orientation of external electric field due to the larger space endowed by the size increase of free volume holes in PVDF/AO composites, leading to more sufficient orientation polarization.

holes and confirms the plausible interpretation of larger dielectric constant than the theoretical value. The positive effect of free volume holes is diagramed in Scheme 2. As shown, the dipoles are randomly oriented, the orientation of which is constricted by small free volume holes, hence the orientation polarization is insufficient. In PVDF/AO composite with larger free volume holes, intrinsic dipoles are more parallel to the orientation of external electric field due to the larger space endowed by the size increment of free volume holes, leading to more sufficient orientation polarization and finally higher dielectric constant than the theoretical value.

For further confirming the dielectric constant enhancement at 10^3 Hz, the *P–E* loops of PVDF/AO composites are collected at 100 MV m^{-1} and displayed in Fig. 4(a). It is shown that the polarization strength of PVDF/AO composites is greatly enhanced as the AO content increases, which confirms the improved dielectric constant. The dielectric constant at 1 kHz and maximal polarization strength P_{max} of PVDF/AO composites *versus* the filler loading are displayed in Fig. 4(b), which indicates the enhanced maximum polarization strength originates from the improved dielectric constant.

Typically, the dielectric constant of polymer nanocomposites will obviously decline due to the suppressed interfacial polarization with the increment of frequency. However, as presented in Fig. 3(a), with frequency increasing, the dielectric constant of PVDF/AO composites with high AO loading is even far smaller than that of PVDF/AO with low AO content, which is not merely ascribed to the suppressed interfacial polarization, and the orientation polarization should be equally considered. As PVDF is a kind of HESD polymer at room temperature, the high dielectric constant mainly stems from the orientation polarization and its free volume is relatively larger than that of the
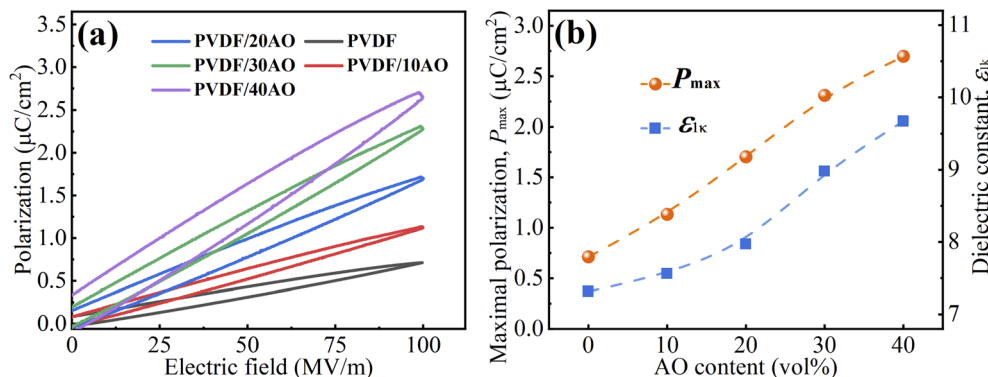
Fig. 4 (a) Polarization–electric field loops of pristine PVDF and PVDF/AO composites. (b) Maximal polarization strength and dielectric constant in PVDF/AO composites, displaying unified increase *versus* AO content. The line in (b) is drawn to guide eyes.

glass-state polymer. Moreover, the orientation polarization will also be greatly restricted under increased frequency.[53] In this situation, the positive effect of free volume tends to be greatly constrained. The increase of free volume could decrease the number of dipoles per unit volume, which could be clarified by the following Debye equation:[54]

$$\frac{\varepsilon - 1}{\varepsilon + 2} = \frac{4\pi}{3} N \left(\alpha_e + \alpha_d + \frac{\mu^2}{3k_B T} \right) \quad (4)$$

where ε is the dielectric constant of the materials, N is the number of dipoles per unit volume, α_e is the polarization of electrons, α_d is the distortion polarization, k_B is the Boltzmann constant, T is the temperature and μ is the dipole moment related to orientation polarization.

According to eqn (4), with the increased free volume hole size in PVDF/AO composites, the dipole density of PVDF will be reduced, which means the decrease of N value,[55] and the decrease of N will consequently contribute to the decline of dielectric constant. In other words, at high frequency, with the greatly weakened orientation polarization of intrinsic dipoles, the dipolar PVDF can be regarded as a kind of non-polar or weak polar polymer, thus the dielectric constant will certainly decrease due to the reduced dipole density brought by the size increment of free volume holes. This explains the rapid decreasing dielectric constant with the increased size of free

volume holes under high frequency, and this is the negative effect of free volume holes at high frequency.

To confirm the negative effect of free volume holes, the theoretical dielectric constant at 10 MHz is estimated and compared with the corresponding experimental dielectric constant, shown in Fig. 5(a). It can be observed, different from the comparison at 1 kHz, the experimental dielectric constant of PVDF/AO composites at 10 MHz is much smaller than the theoretical value, which is obviously not only ascribed to the weakening of interfacial polarization but also the negative effect of free volume holes on dielectric constant.

Especially, an intersection region of the dielectric spectrums for PVDF nanocomposite films is observed between 10^3 and 10^4 Hz in Fig. 3(a). This intersection region is considered the balanced range of positive and negative effects of free volume holes on the dielectric constant. At frequency lower than this, the positive effect is dominant but the negative effect is prominent at frequency higher than this region. Considering the discussions and conclusions in previous works,[14–20] it is concluded that the free volume effects (positive or negative) depend on the type of polymer (polar or non-polar), intrinsic free volume level and the frequency.

The frequency dependence of dielectric constant of PVDF/AO composite films is also discussed. The decrease $\Delta\varepsilon$ and reduction rate $R_{\Delta\varepsilon}$ of dielectric constant, defined as $\Delta\varepsilon = \varepsilon_{1k} - \varepsilon_{10M}$
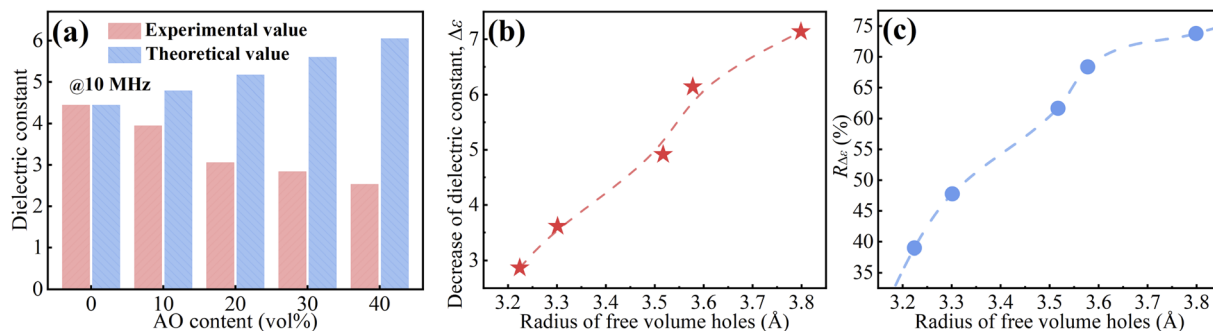

Fig. 5 (a) Comparison of experimental dielectric constant and theoretical dielectric constant of PVDF/AO composite films at 10 MHz. (b) Correlation of decrease of dielectric constant and free volume radius. (c) Correlation of decrease rate of dielectric constant and free volume radius in PVDF/AO composites. The lines are drawn to guide eyes.

and $R_{\Delta\varepsilon} = (\varepsilon_{1k} - \varepsilon_{10M})/\varepsilon_{1k}$, are obtained and exhibited in Fig. 5(b) and (c). It is shown that the decrease and reduction ratio of dielectric constant all exhibit remarkable dependence on the radius of free volume holes. The frequency dependence is more intense with the size increment of free volume holes. As discussed above, in addition to interfacial polarization, the free volume effects caused by the radius variation of free volume holes also account for the stronger frequency dependence of dielectric constant in PVDF/AO composites.

4. Conclusion

In summary, the free volume of dipolar PVDF is regulated by the addition of Al_2O_3 and the free volume effects on dielectric constant of PVDF/Al_2O_3 composites are discussed, which are believed to tightly depend on the polymer type (polar or non-polar), intrinsic free volume level and the frequency. The free volume holes tend to generate dual effects on the dielectric constant of PVDF nanocomposites. The larger experimental dielectric constant of PVDF than the theoretical value at low frequency is attributed to the positive effect of free volume holes, namely the strengthened orientation polarization of intrinsic dipoles. On the other hand, the much lower experimental dielectric constant than the theoretical value at high frequency is believed to originate from the negative effect of free volume holes, namely the decrease of dipole density and restriction on orientation polarization due to frequency increasing. Consequently, in such kind of HESD polymer, the dual effects of free volume holes on dielectric constant of PVDF/Al_2O_3 composites under low and high frequencies tend to account for the remarkable frequency dependence of dielectric constant. The atomic-scale microstructure analysis based on free volume provides valuable understanding and novel insights for the study of mechanism of dielectric behaviour of polymer composites and is favorable for further optimizing the dielectric properties of dipolar dielectric polymer-based composites.

Author contributions

Lei Yang: visualization, investigation, writing original draft. Xuyang Liu: investigation, preparation. Zhouxun Lu: investigation, methodology. Tong Song: conceptualization. Zhihong Yang: supervision. Jianmei Xu: conceptualization. Wei Zhou: supervision, conceptualization, writing – review & editing. Xingzhong Cao: methodology. Runsheng Yu: review & editing. Qing Wang: review & editing.

Conflicts of interest

The authors declare that they have no known competing financial interests or personal relationships that could have appeared to influence the work reported in this paper.

Acknowledgements

References

1 B. Luo, X. Wang, Y. Wang and L. Li, Fabrication, characterization, properties and theoretical analysis of ceramic/PVDF composite flexible films with high dielectric constant and low dielectric loss, *J. Mater. Chem. A*, 2014, **2**(2), 510–519.

2 B. Chu, X. Zhou, K. Ren, B. Neese, M. Lin, Q. Wang, F. Bauer and Q. M. Zhang, A dielectric polymer with high electric energy density and fast discharge speed, *Science*, 2006, **313**(5785), 334–336.

3 P. Thomas, S. Satapathy, K. Dwarakanath and K. B. R. Varma, Dielectric properties of poly(vinylidene fluoride)/$CaCu_3Ti_4O_{12}$ nanocrystal composite thick films, *eXPRESS Polym. Lett.*, 2010, **4**(10), 632–643.

4 Y. Wu, X. Lin, X. Shen, X. Sun, X. Liu, Z. Wang and J.-K. Kim, Exceptional dielectric properties of chlorine-doped graphene oxide/poly (vinylidene fluoride) nanocomposites, *Carbon*, 2015, **89**, 102–112.

5 Prateek, V. K. Thakur and R. K. Gupta, Recent Progress on Ferroelectric Polymer-Based Nanocomposites for High Energy Density Capacitors: Synthesis, Dielectric Properties, and Future Aspects, *Chem. Rev.*, 2016, **116**(7), 4260–4317.

6 H. H. Wu, F. P. Zhuo, H. M. Qiao, L. K. Venkataraman, M. P. Zheng, S. Z. Wang, H. Huang, B. Li, X. P. Mao and Q. B. Zhang, Polymer-/Ceramic-based Dielectric Composites for Energy Storage and Conversion, *Energy Environ. Mater.*, 2022, **5**(2), 486–514.

7 S. Kumar, S. Supriya and M. Kar, Enhancement of dielectric constant in polymer-ceramic nanocomposite for flexible electronics and energy storage applications, *Compos. Sci. Technol.*, 2018, **157**, 48–56.

8 Z. M. Dang, M. S. Zheng and J. W. Zha, 1D/2D Carbon Nanomaterial-Polymer Dielectric Composites with High Permittivity for Power Energy Storage Applications, *Small*, 2016, **12**(13), 1688–1701.

9 Y. F. Wang, J. Cui, Q. B. Yuan, Y. J. Niu, Y. Y. Bai and H. Wang, Significantly Enhanced Breakdown Strength and Energy Density in Sandwich-Structured Barium Titanate/Poly(vinylidene fluoride) Nanocomposites, *Adv. Mater.*, 2015, **27**(42), 6658–6663.

10 Z. Shi, J. Wang, F. Mao, C. Yang, C. Zhang and R. Fan, Significantly improved dielectric performances of sandwich-structured polymer composites induced by alternating positive-k and negative-k layers, *J. Mater. Chem. A*, 2017, **5**(28), 14575–14582.

11 T. D. Zhang, L. Y. Yang, C. H. Zhang, Y. Feng, J. Wang, Z. H. Shen, Q. G. Chen, Q. Q. Lei and Q. G. Chi, Polymer dielectric films exhibiting superior high-temperature

capacitive performance by utilizing an inorganic insulation interlayer, *Mater. Horiz.*, 2022, **9**(4), 1273–1282.

12 Y. K. Zhu, Y. J. Zhu, X. Y. Huang, J. Chen, Q. Li, J. L. He and P. K. Jiang, High Energy Density Polymer Dielectrics Interlayered by Assembled Boron Nitride Nanosheets, *Adv. Energy Mater.*, 2019, **9**, 1901826.

13 C. Chen, T. D. Zhang, C. H. Zhang, Y. Feng, Y. Q. Zhang, Y. Zhang, Q. G. Chi, X. Wang and Q. Q. Lei, Improved Energy Storage Performance of P(VDF-TrFE-CFE) Multilayer Films by Utilizing Inorganic Functional Layers, *ACS Appl. Energy Mater.*, 2021, **4**(10), 11726–11734.

14 Q. Y. Zhang, X. Chen, T. Zhang and Q. M. Zhang, Giant permittivity materials with low dielectric loss over a broad temperature range enabled by weakening intermolecular hydrogen bonds, *Nano Energy*, 2019, **64**, 103916.

15 T. Zhang, X. Chen, Y. Thakur, B. Lu, Q. Y. Zhang, J. Runt and Q. M. Zhang, A highly scalable dielectric metamaterial with superior capacitor performance over a broad temperature, *Sci. Adv.*, 2020, **6**, eaax6622.

16 F. Fu, M. G. Shen, D. Wang, H. Liu, S. B. Shang, F. L. Hu, Z. Q. Song and J. Song, A rosin-based dielectric polymer with intrinsic low dielectric constant and comprehensively excellent properties, *J. Mater. Chem. C*, 2021, **9**(38), 13144–13156.

17 B. S. Liu, K. G. Haw, C. Zhang, G. L. Yu, J. L. Li, P. P. Zhang, S. Y. Li, S. Wu, J. Y. Li and X. Q. Zou, Flexible films derived from PIM-1 with ultralow dielectric constants, *Microporous Mesoporous Mater.*, 2020, **294**, 109887.

18 J. Lin and X. Wang, Novel low-κ polyimide/mesoporous silica composite films: Preparation, microstructure, and properties, *Polymer*, 2007, **48**(1), 318–329.

19 T. M. Long and T. M. Swager, Molecular design of free volume as a route to low-kappa dielectric materials, *J. Am. Chem. Soc.*, 2003, **125**(46), 14113–14119.

20 M.-H. Tsai and W.-T. Whang, Low dielectric polyimide/poly (silsesquioxane)-like nanocomposite material, *Polymer*, 2001, **42**(9), 4197–4207.

21 R. Gregorio and E. M. Ueno, Effect of crystalline phase, orientation and temperature on the dielectric properties of poly (vinylidene fluoride) (PVDF), *J. Mater. Sci.*, 1999, **34**(18), 4489–4500.

22 A. K. Doolittle, Studies in Newtonian Flow. II. The Dependence of the Viscosity of Liquids on Free-Space, *J. Appl. Phys.*, 1951, **22**(12), 1471–1475.

23 E. Henry, Viscosity, Plasticity, and Diffusion as Examples of Absolute Reaction Rates, *J. Chem. Phys.*, 1936, **4**(4), 283–291.

24 T. G. Fox and P. J. Flory, Second-Order Transition Temperatures and Related Properties of Polystyrene. I. Influence of Molecular Weight, *J. Appl. Phys.*, 1950, **21**(6), 581–591.

25 V. Gaydarov, Z. Y. Chen, G. Zamfirova, M. A. Soylemez, J. M. Zhang, N. Djourelov and J. Zhang, Micromechanical and positron annihilation lifetime study of new cellulose esters with different topological structures, *Carbohydr. Polym.*, 2019, **219**, 56–62.

26 M. Nuruddin, R. A. Chowdhury, R. Lopez-Perez, F. J. Montes, J. P. Youngblood and J. A. Howarter, Influence of Free Volume Determined by Positron Annihilation Lifetime Spectroscopy (PALS) on Gas Permeability of Cellulose Nanocrystal Films, *ACS Appl. Mater. Interfaces*, 2020, **12**(21), 24380–24389.

27 H. J. Zhang, S. Sellaiyan, K. Sako, A. Uedono, Y. Taniguchi and K. Hayashi, Effect of free-volume holes on static mechanical properties of epoxy resins studied by positron annihilation and PVT experiments, *Polymer*, 2020, **190**, 122225.

28 I. Irska, S. Paszkiewicz, D. Pawlikowska, J. Dryzek, A. Linares, A. Nogales, T. A. Ezquerra and E. Piesowicz, Relaxation behaviour and free volume of bio-based Poly(trimethylene terephthalate)-*block*-poly(caprolactone) copolymers as revealed by Broadband Dielectric and Positron Annihilation Lifetime Spectroscopies, *Polymer*, 2021, **229**, 123949.

29 D. Ponnamma, R. Ramachandran, S. Hussain, R. Rajaraman, G. Amarendra, K. T. Varughese and S. Thomas, Free-volume correlation with mechanical and dielectric properties of natural rubber/multi walled carbon nanotubes composites, *Composites, Part A*, 2015, **77**, 164–171.

30 M. Lei, Y. J. Wang, C. Liang, K. Huang, C. X. Ye, W. J. Wang, S. F. Jin, R. Zhang, D. Y. Fan, H. J. Yang and Y. G. Wang, Positron annihilation lifetime study of Nafion/titanium dioxide nano-composite membranes, *J. Power Sources*, 2014, **246**, 762–766.

31 P. Kirkegaard, M. Eldrup, O. E. Mogensen and N. J. Pedersen, Program system for analysing positron lifetime spectra and angular correlation curves, *Comput. Phys. Commun.*, 1981, **23**(3), 307–335.

32 L. M. Liu, P. F. Fang, S. P. Zhang and S. J. Wang, Effect of epoxide equivalent on microstructure of epoxy/rectorite nanocomposite studied by positrons, *Mater. Chem. Phys.*, 2005, **92**(2–3), 361–365.

33 S. J. Tao, Positronium annihilation in molecular substances liquids and solids, *J. Chem. Phys.*, 1972, **56**(11), 5499–5510.

34 M. Eldrup, D. Lightbody and J. N. Sherwood, The temperature dependence of positron lifetimes in solid pivalic acid, *Chem. Phys.*, 1981, **63**(1–2), 51–58.

35 H. Nakanishi, S. Wang and Y. Jean, *Positron Annihilation Studies of Fluids*, World Science, Singapore, 1988, p. 292.

36 Y. Feng, W. L. Li, J. P. Wang, J. H. Yin and W. D. Fei, Core-shell structured $BaTiO_3$@carbon hybrid particles for polymer composites with enhanced dielectric performance, *J. Mater. Chem. A*, 2015, **3**(40), 20313–20321.

37 Y. L. Su, Y. Q. Gu and S. N. Feng, Composites of NBCTO/MWCNTs/PVDF with high dielectric permittivity and low dielectric loss, *J. Mater. Sci.: Mater. Electron.*, 2018, **29**(3), 2416–2420.

38 W. B. Zhang, Z. X. Zhang, J. H. Yang, T. Huang, N. Zhang, X. T. Zheng, Y. Wang and Z. W. Zhou, Largely enhanced thermal conductivity of poly(vinylidene fluoride)/carbon nanotube composites achieved by adding graphene oxide, *Carbon*, 2015, **90**, 242–254.

39 X. Xie, M. B. Zhou, L. Q. Lv, S. Y. Liu and J. Shen, The fabrication of the ultra-thin polyvinylidene fluoride

dielectric films for nanoscale high energy density capacitors, *Polymer*, 2017, **132**, 193–197.

40 S. Dash, R. N. P. Choudhary and M. N. Goswami, Enhanced dielectric and ferroelectric properties of PVDF-BiFeO3 composites in 0-3 connectivity, *J. Alloys Compd.*, 2017, **715**, 29–36.

41 J. Asaad, E. Gomaa and I. K. Bishay, Free-volume properties of epoxy composites and its relation to macrostructure properties, *Mater. Sci. Eng., A*, 2008, **490**(1–2), 151–156.

42 B. Zhang, X. Chen, W. C. Lu, Q. M. Zhang and J. Bernholc, Morphology-induced dielectric enhancement in polymer nanocomposites, *Nanoscale*, 2021, **13**(24), 10933–10942.

43 J. Fan, W. Zhou, Q. Wang, Z. Chu, L. Yang, L. Yang, J. Sun, L. Zhao, J. Xu, Y. Liang and Z. Chen, Structure dependence of water vapor permeation in polymer nanocomposite membranes investigated by positron annihilation lifetime spectroscopy, *J. Membr. Sci.*, 2018, **549**, 581–587.

44 W. Zhou, J. Wang, Z. Gong, J. Gong, N. Qi and B. Wang, Investigation of interfacial interaction and structural transition for epoxy/nanotube composites by positron annihilation lifetime spectroscopy, *Appl. Phys. Lett.*, 2009, **94**(2), 021904.

45 P. Winberg, K. De Sitter, C. Dotremont, S. Mullens, I. F. J. Vankelecom and F. H. J. Maurer, Free volume and interstitial mesopores in silica filled poly(I-trimethylsilyl-l-propyne) nanocomposites, *Macromolecules*, 2005, **38**(9), 3776–3782.

46 Z. M. Dang, H. P. Xu and H. Y. Wang, Significantly enhanced low-frequency dielectric permittivity in the BaTiO₃/poly(vinylidene fluoride) nanocomposite, *Appl. Phys. Lett.*, 2007, **90**, 012901.

47 J. L. Li, J. H. Yin, C. Yang, N. Li, Y. Feng, Y. Y. Liu, H. Zhao, Y. P. Li, C. C. Zhu, D. Yue, B. Su and X. X. Liu, Enhanced dielectric performance and energy storage of PVDF-HFP-based composites induced by surface charged Al₂O₃, *J. Polym. Sci., Part B: Polym. Phys.*, 2019, **57**(10), 574–583.

48 Z. M. Dang, J. K. Yuan, J. W. Zha, T. Zhou, S. T. Li and G. H. Hu, Fundamentals, processes and applications of high-permittivity polymer matrix composites, *Prog. Mater. Sci.*, 2012, **57**(4), 660–723.

49 N. Jayasundere and B. V. Smith, Dielectric-constant for binary piezoelectric 0-3 composites, *J. Appl. Phys.*, 1993, **73**(5), 2462–2466.

50 C. L. Huang, J. J. Wang and C. Y. Huang, Sintering behavior and microwave dielectric properties of nano alpha-alumina, *Mater. Lett.*, 2005, **59**(28), 3746–3749.

51 Z. F. Wang, B. Wang, X. M. Ding, M. Zhang, L. M. Liu, N. Qi and J. L. Hu, Effect of temperature and structure on the free volume and water vapor permeability in hydrophilic polyurethanes, *J. Membr. Sci.*, 2004, **241**(2), 355–361.

52 B. Wang, Z. F. Wang, M. Zhang, W. H. Liu and S. J. Wang, Effect of temperature on the free volume in glassy poly(ethylene terephthalate), *Macromolecules*, 2002, **35**(10), 3993–3996.

53 H. Li, Y. Zhou, Y. Liu, L. Li, Y. Liu and Q. Wang, Dielectric polymers for high-temperature capacitive energy storage, *Chem. Soc. Rev.*, 2021, **50**(11), 6369–6400.

54 W. Volksen, R. D. Miller and G. Dubois, Low Dielectric Constant Materials, *Chem. Rev.*, 2010, **110**(1), 56–110.

55 G. Hougham, G. Tesoro and A. Viehbeck, Influence of free volume change on the relative permittivity and refractive index in fluoropolyimides, *Macromolecules*, 1996, **29**(10), 3453–3456.